Histol Histopath (1992) 7: 267-273

Histology and Histopathology

Morphology of epiphyseal apparatus of a ranid frog (*Rana Esculenta*)

Carlo Dell'Orbo[1], Luciana Gioglio[2] and Daniela Quacci[1]
[1]Department of Cytomorphology, University of Cagliari and [2]Institute of Human Anatomy, University of Pavia, Italy

Summary. Morphological, histochemical and ultrastructural investigations on epiphyseal apparatus of *Rana Esculenta* were made. The most important findings were the following: 1) metaphyseal cartilage is localized inside proximal diaphyseal compact bone as a plug; 2) metaphyseal cartilage do not reduce in thickness during ageing; 3) metaphyseal cartilage do not show vascular invasion and do not mineralize in degenerative zone; 4) trabecular bone was not at all evident in this animal; 5) external periosteum is well vascularized and proliferates in correspondence to marginal epiphyseal end of the diaphyseal.

From these results the hypothesis that the ranid frog bone growth is not due to metaphyseal metabolism (as in avian and mammals) but to bone periosteal marginal mineralization is reached.

Key words: Epiphysis, Bone growth, Ranid frog

Introduction

The mammalian epiphyseal apparatus has been extensively investigated either by light microscopy (Jee, 1986), or electron microscopy (Thyberg et al., 1973; Landis and Hodgens, 1990; Quacci et al., 1990) and biochemical methods (Stagni et al., 1979; De Bernard et al., 1986) and thus a relatively codified «theory of growth» of epiphyseal apparatus may be postulated now.

The amphibian epiphyseal apparatus has hardly been studied (Frobose, 1927; Dickson, 1982), but the absence of the vascular invasion in epiphyseal plate (Dickson, 1978), which is the starting factor of mammalian calcification and bone ingrowth (Anderson and Parker, 1966; Hunter and Arsenault, 1990), make probable a particular bone growing mechanism in amphibians.

So further morphological investigations on amphibian epiphyseal apparatus are necessary to attempt to explain the growth of long bones.

Offprint requests to: Prof. Daniela Quacci, Dipartimento di Citomorfologia, via Porcell 2, I-09124 Cagliari, Italy

Materials and methods

Several stocks of frogs (*Rana Esculenta*) were purchased from a local supplier and kept in an aquarium for 10 - 15 days. The age of the animals was unknown, and consequently they were classified according to their body weight (range 6 to 36 g).

Each specimen was anaesthetized by dipping it in a 1/1000 solution of MS 222 Sandoz. The femoral proximal metaphyses were quickly dissected from the surrounding soft tissues, cut lengthwise in two halves, examined with a stereo-microscope and photographed.

The specimens were then prepared for examination by light and electron microscopy.

After a short primary fixation, in the solutions listed below, the metaphyseal cartilages were dissected longitudinally in order to obtain small fragments for a better penetration of fixative solutions.

Light microscopy

The specimens were fixed in Bouin's solution, decalcified in 4% aqueous formic acid for 2 days, dehydrated in ascending concentrations of cold ethanol and xylene and embedded in paraffin.

The sections of about 7 - 10 μm were stained with Eosin-Haematoxylin, Azan, PAS and Von Kossa reactions according to Pearse (1980), and Alcian blue dissolved in $MgCl_2$ critical electrolitic concentration (C.E.C.) solutions following Scott and Dorling (1965). All stained sections were mounted in resin and observed and photographed by a Leitz Orthoplan.

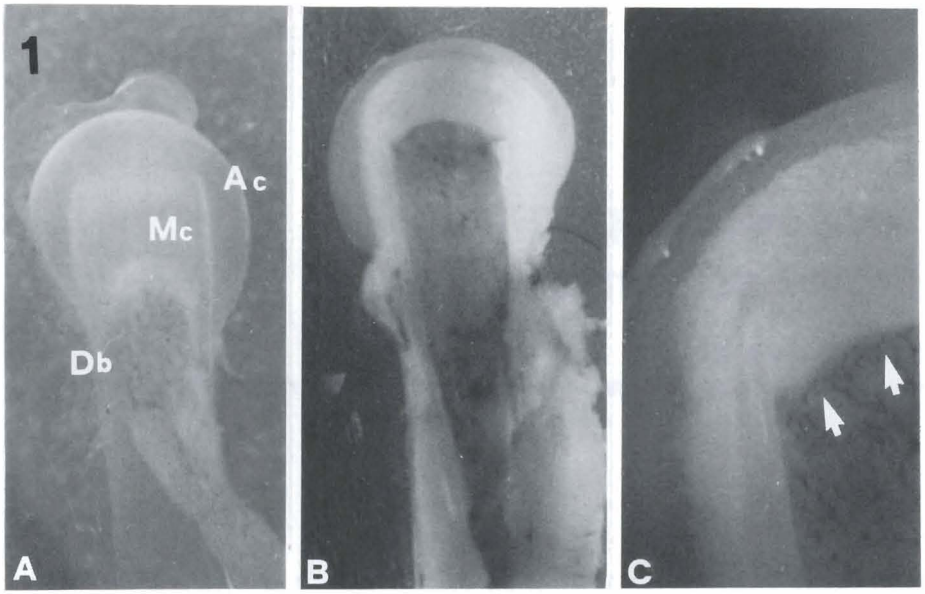

Fig. 1. Epiphyseal apparatus of proximal femur. **A.** body weight 6 g (× 10). The articular cartilage (Ac) and metaphyseal cartilage (Mc) appear as white transparent tissue and diaphyseal bone (Db) is easily recognizable as white opaque material. Metaphyseal cartilage is localized inside proximal diaphyseal compact bone as a plug. The epiphyseal calcification nucleus is completely lacking. **B.** Body weight 36 g (× 20). The thickness of metaphyseal cartilage is unvaried. **C.** Body weight 36 g (× 40). Deeper articular zones have a frosted glass aspect. The bone marrow vessels (red-brown colour) run prevalently parallel to diaphyseal long axis but near to the metaphyseal cartilage they go in a perpendicular way, running parallel to the inner metaphysis (arrow).

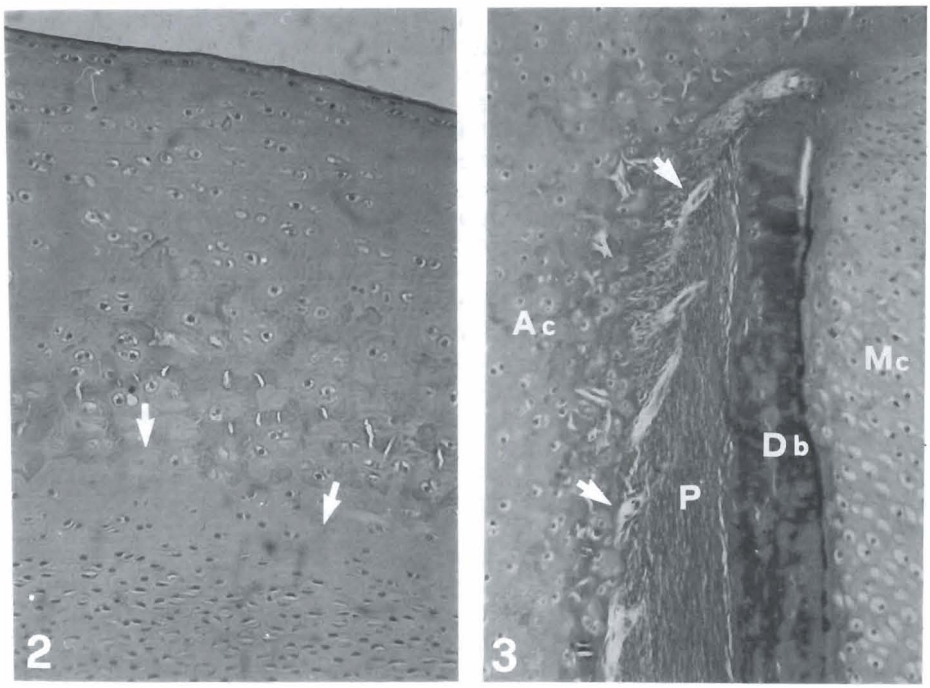

Fig. 2. Articular cartilage. (× 200). Azan. The superficial-zone chondrocytes are elongated in shape. The deeper zone ones become rounded and lie directly on the resting zone of the metaphyseal cartilage (arrow).

Fig. 3. Diaphyseal edge. (× 200). Azan. Diaphyseal edge (D) and its periostium (P) are respectively limited by metaphyseal cartilage (Mc) and articular cartilage (Ac). Periosteal vessels are transversely sectioned.

Electron microscopy

Some metaphyseal cartilage fragments were fixed in 4% glutaraldehyde in Millonig's amphibian phosphate buffer, pH 7.35, for 12 hr. The specimens were then washed in the same buffer.

All specimens were then postfixed in 1% osmium tetroxide solution in 0.1 M phosphate buffer at pH 7.4, dehydrated in ascending concentrations of cold ethanol, passed through cold propyleneoxide and embedded in Epon. Ultrathin sections cut with a Reichert OM 12 ultramicrotome, were collected on 300 mesh copper or gold grids.

Some sections were collected on gold grids and decalcified with ethylene-diamine-tetra-acetic acid (EDTA) dissolved in water or in alcoholic solution (Scott and Burton, 1984).

Some grids were stained either with uranyl acetate-lead citrate (Reynolds, 1963) or uranyl acetate-sodium bismuth, (Riva, 1974) and examined with a Jeol 100S EM.

Results

Macro-anatomy

The epiphyseal apparatus was constituted by articular cartilage, metaphyseal cartilage, boundary zone and diaphyseal bone with its periosteum. Bone, cartilage and vessels were easily distinguishable in rana proximal femur.

At low enlargement (ten times) the articular and metaphyseal cartilage appeared as white transparent tissue. Diaphyseal bone was easily recognizable as a white opaque one and vessels had a red-brown colour. Diaphyseal bone went into the epiphysis and separated metaphyseal from articular cartilage (Fig. 1A). The articular cartilage surrounded and enveloped the diaphysis and metaphyseal cartilage.

Metaphyseal cartilage was localized inside proximal

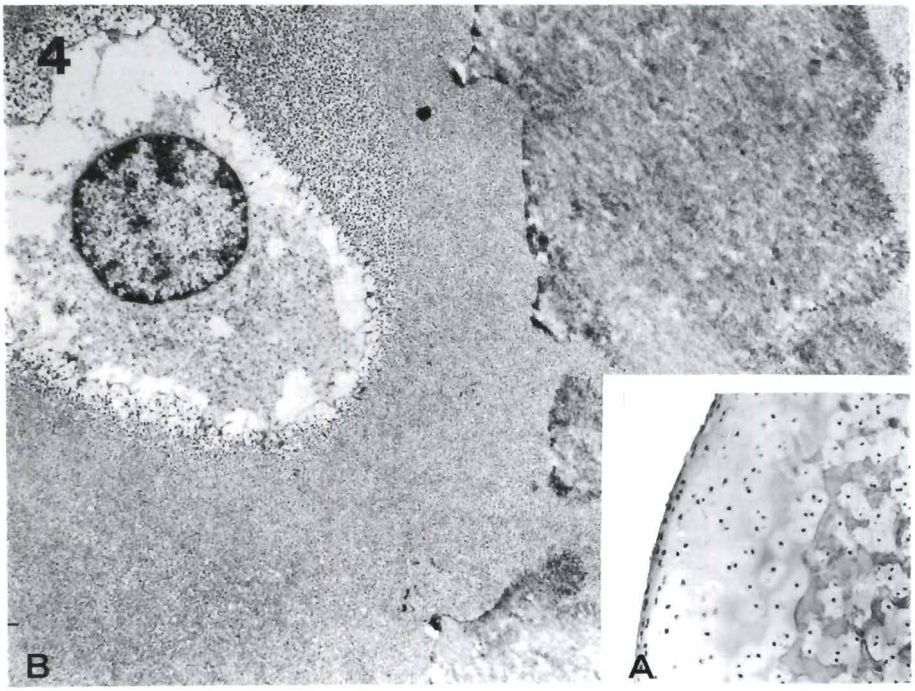

Fig. 4. Articular cartilage. **A.** (× 50). Haematoxylin-Eosin. In older specimens the interterritorial matrix presents a mottled aspect corresponding to the progressive mineralization of these layers. **B.** (× 8,000). At ultrastructural observation the mineralized zone shows some strongly electrondense, needle-like particles, ultrastructural evidence of hydroxyapathite crystals, coming together and forming the mineralizing front.

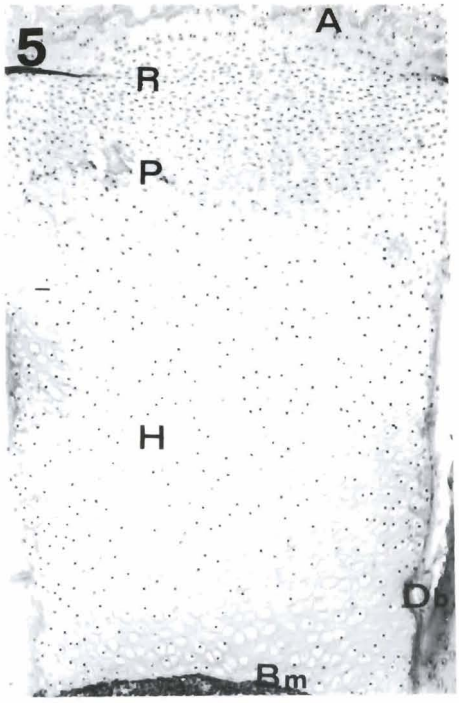

Fig. 5. Metaphyseal cartilage (× 120). Haematoxylin-Eosin. The metaphyseal cartilage may be divided into reserve (R), proliferative (P) and hypertrophic (H) zones. Articular cartilage (Ac), Diaphyseal bone (Db), Bone marrow (Bm).

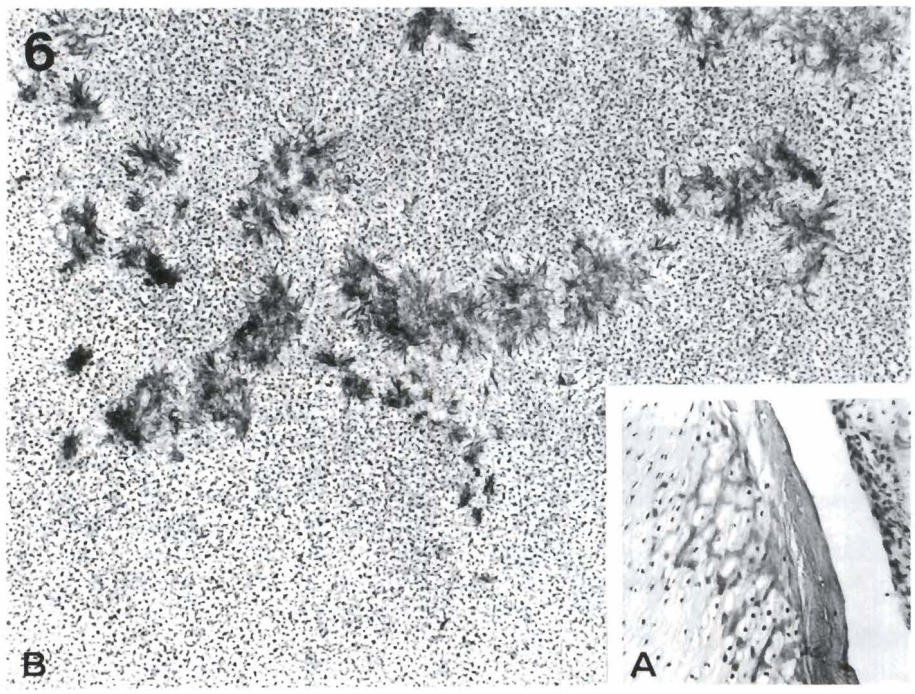

Fig. 6. Metaphyseal wedge-shaped area. **A.** (× 50). Hematoxylin-eosin. A circular mineralized wedge-shaped area can be detected in the oldest animals inside the proliferative zone. **B.** (× 18,000). At electron microscopic level, in all metaphyseal zones, the matrix presents collagen fibrils and matrix granules, which are sometime masked by a lot of electronopaque needle-like crystals.

diaphyseal compact bone as a plug. The epiphyseal calcification nucleus was completely lacking (Fig. 1A).

The metaphyseal cartilage was present in the older animal, too, and its thickness does not vary during ageing (Fig. 1B).

The diaphysis diameter (1.2 mm. in 6 g Ranae) enlarged about three times during animal growth (3.1 mm in 36 g Ranae) but the diaphyseal bone marrow cavity did not enlarge.

In the older frogs deeper articular cartilage lost its transparency and presented a frosted glass aspect (Fig. 1B).

The metaphyseal cartilage maintained the transparent aspect in the oldest animals also. The contact plane between bone marrow and cartilage presented a concavity to bone marrow.

The diaphyseal bone marrow vessels ran prevalently parallel to diaphyseal long axis but near to the metaphyseal cartilage they went in a perpendicular way, running parallel to the inner metaphyseal surface (Fig. 1C). The vessel architecture

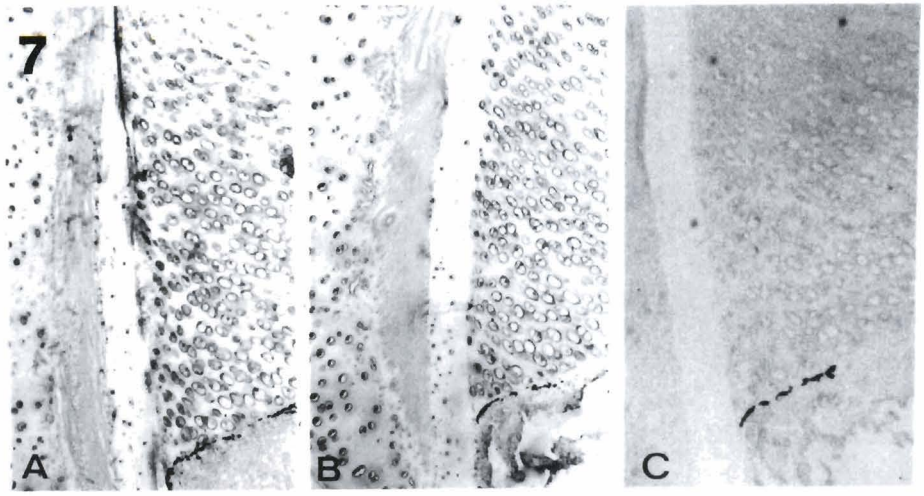

Fig. 7. Alcian blue stains (× 80). A: 0.05 M; B: 0.3 M and C: 0.6 M $MgCl_2$. In the metaphyseal zone from proliferative to hypertrophic zone no stain variation is evident. The increased concentration of $MgCl_2$ to 0.6 M completely avoids Alcian blue staining.

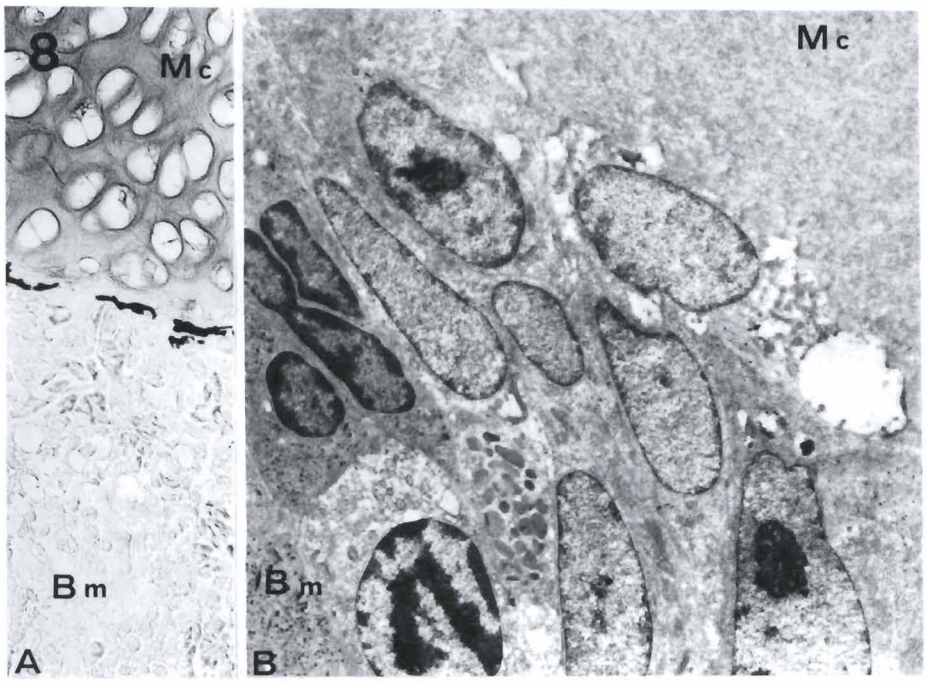

Fig. 8. Boundary zone. **A.** (× 600). Haematoxylin-eosin. The boundary zone is characterized by a continous layer of dark cells separating the metaphysis (Mc) from bone marrow (Bm). **B.** (× 3,500). The lining cells present two morphological aspects: either as elongated cells, very similar to bone lining cells with a cytoplasm very poor in cytoplasmic organelles, or as globular cells with a diffuse rough reticulum and a large amount of small dark vesicles.

did not present significative modifications during ageing.

Micro-anatomy, histochemistry, ultrastructure

Articular cartilage

The chondrocytes of the superficial zone were more numerous than elsewhere in articular cartilage (Fig. 2). They were discoidal cells flattened in a plane parallel to the articular surface and in longitudinal sections they appeared elongated in shape. The deeper zone chondrocytes became rounded and their number decreased. The deeper zone of articular cartilage lay directly on the resting zone of the metaphyseal cartilage. In older specimens to interterritorial matrix became more stainable to Haematoxylin (Fig. 4A) and presented a mottled aspect in correspondence to the progressive mineralization of these layers. The better-mineralized areas were red to Azan stain. The deeper articular zone evidenced a diffuse black-brown Von Kossa staining in older animals.

0.3M $MgCl_2$ Alcian blue stained the deeper chondrocyte lacunar sinus, but the superficial ones were completely unstained. At 0.6 M $MgCl_2$ Alcian blue all articular cartilage was completely unstained.

The staining reactions were suggestively similar in young and older animals. This may mean that ageing and progressive mineralization do not affect staining properties.

At ultrastructural observation the mineralized zone showed some needle-like particles, ultrastructural evidence of hydroxyapatite crystals, coming together and forming the mineralizing front. The mineralization invaded the cartilage matrix masking either collagen fibrils or matrix granules, ultrastructural evidence of proteoglycan aggregates (Fig. 4B).

Metaphyseal cartilage

The metaphyseal cartilage may be divided in reserve, proliferative and hypertrophic zones and it was limited, contained and in direct contact with the inner diaphyseal bone surface. The hypertrophic zone was in contact with the bone diaphyseal marrow through a fourth zone: the boundary zone (Dickson, 1982) (Figs. 3, 5).

The reserve zone was in direct contact with deeper articular cartilage and showed chondrocytes of discoidal shape.

The proliferative zone did not show an ordered columnar organization, but the cells were enlarged and rounded.

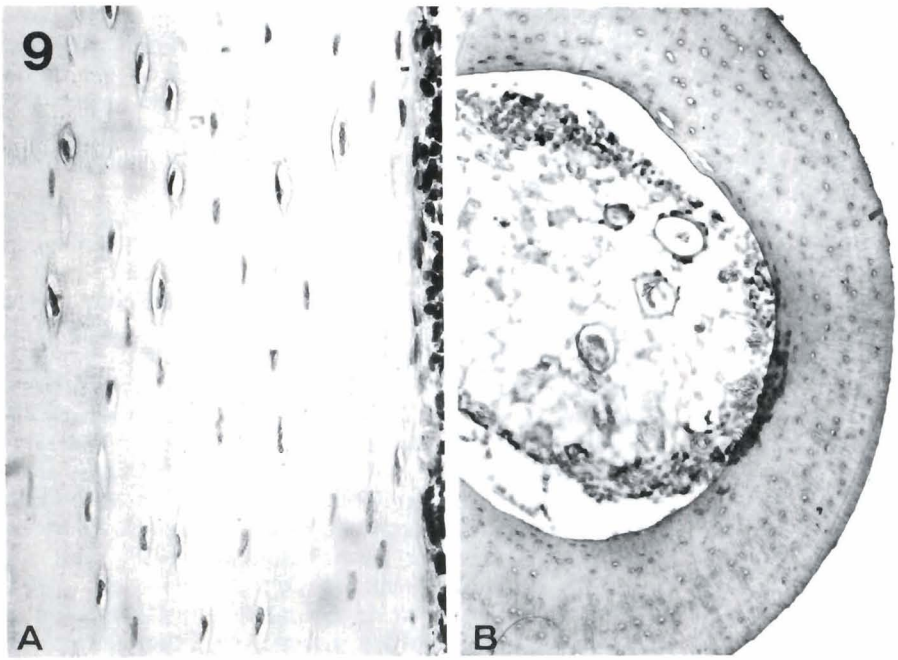

Fig. 9. Diaphyseal bone. Haematoxylin-eosin. **A.** (× 600). Diaphyseal bone is composed of lamellae strictly packed to each other: each lamella is composed of a cell lamina entombed in a mineralized matrix. **B.** (× 200). In transverse sections no osteonic structure could be detected.

The hypertrophic zone showed very large lacunae containing the chondrocytes. No vascular invasion could be detected from the bone marrow through the borderline zone into the metaphyseal territory (Figs. 5, 8A).

A ring-like mineralized wedge-shaped area could be detected in the oldest animals inside the proliferative zone (Fig. 6A): Von Kossa staining confirmed the presence of calcium salts in this zone.

Alcian blue in C.E.C. solution stains did not show any variation, in the metaphyseal zone, from proliferative to hypertrophic zone, and the increasing concentration of $MgCl_2$ to 0.6M completely avoided Alcian blue staining in the whole metaphysis (Figs. 7A, 7B, 7C).

At ultrastructural observations, the matrix presented collagen fibrils, not over 40 nm in diameter and with a regular periodicity of 68 nm, and matrix granules, morphological expression of cartilage proteoglycans, whose diameter was 14 nm. No collagen and matrix granule shape and diameter variations from reserve to hypertrophic could be detected. In proliferative wedge-shaped area calcified collagen fibrils and Matrix granules were masked by many electronopaque needle-like crystals (Fig. 6B). Collagen fibrils and matrix granules were completely free from mineralization in all other metaphyseal regions (particularly in hypertrophic region).

Boundary zone

The boundary zone was characterized by the presence of a continuous layer of dark cells (melanocytes?) between the metaphysis and the bone marrow. The dark cells were in close contact with bone marrow capillaries and with the cartilage cells on the metaphyseal side (Fig. 8A).

At ultrastructural level of the lining cells presented two morphological aspects: they appeared either as elongated cells, like bone lining cells and characterized by a scarce number of cytoplasmic organelles, or as roundish in shape with a diffuse rough reticulum and a large amount of little dense vesicles of 80 nm in diameter, similar to lysosomes (Fig. 8B).

Diaphysis

The thickness of the diaphyseal compact bone enlarged from 140 μm. (6 g ranae) to about 1000 μm. (36 g ranae).

Compact bone tissue was the only one bone type present. Trabecular and spongy bone were completely lacking. In diaphysis transverse sections no osteonic structure could be detected (Fig. 9A). Diaphyseal bone was composed by parallel lamellae strictly packed to each other. Each lamella was composed by a cell lamina entombed in a mineralized matrix. Only three cell layers were present in younger animals, but in older ones there were about ten cell layers (Fig. 9B).

Endosteum was composed of a thin monolayer of flat epithelial-like cells which separated bone marrow from bone tissue (bone lining cells).

In epiphyseal apparatus the inner bone was in direct contact to metaphyseal cartilage (Fig. 3).

External diaphyseal surface presented the periosteal membrane composed of multiple layers of connective cells enveloped in unmineralized matrix (Fig. 3).

In epiphyseal zone the periosteum was in direct contact with articular cartilage and it thickened at the expense of the diaphyseal bone progressively thinning.

Transverse and longitudinal sections presented a lot of periosteal vessels with spiral disposition reaching the edge of the diaphyseal bone (Fig. 3). This part was covered by enlarged and crowded cells lining the external diaphyseal surface and the diaphyseal edge. The cells were characterized by a well-developed rough endoplasmic reticulum, and Golgi apparatus was localized in the perinuclear area. It was similar to osteoblasts.

The Alcian stain was completely lacking in diaphyseal bone matrix except as a thin pericellular layer (0.3 M $MgCl_2$ Alcian blue). Higher $MgCl_2$ concentrations made completely negative proteoglycan detection with Alcian blue (Figs. 7A, 7B, 7C).

The bone matrix presented a mottled aspect.

At ultrastructural level the limit between bone and metaphyseal cartilage and from bone and bone marrow was very evident. The external surface presented many osteoblast-like cells mineralizing on the surface in contact to bone while internal surface was completely free from mineral deposition.

Discussion

The ranid frog metaphyseal cartilage appears completely different from mammalian and from avian ones. In avians (Howlett, 1979) and mammalians (Thyberg, 1973; Quacci et al., 1990) the epiphyseal ossification nucleus is connected to diaphyseal bone through metaphyseal cartilage which is responsible for bone lengthening. In *Rana Esculenta* the metaphyseal cartilage was present inside the diaphyseal bone: this evidence makes it highly improbable that this organ lengthens the bone.

The thickness of metaphyseal cartilage does not reduce during ageing and in all ages degenerating and calcifying zones are completely lacking. This is totally different from what happens in mammals, where metaphyseal cartilage reduces in thickness and disappears when growth stops (Jee, 1986).

The absolute absence of vascular invasion, in the metaphyseal cartilage, completely deprived the epiphysis of the trabecular and osteonic bone.

The cartilage mineralization was only present in two zones of the epiphyseal apparatus: in deeper articular cartilage and at the periphery of the metaphysis, in the circular mineralized wedge-shaped area. This was demonstrated macroscopically by the frosted glass aspect, microscopically by the mottled matrix, and ultrastructurally by the needle-like confluent structures evident in the matrix.

In mammals and in avians, mineralized cartilage is quickly invaded by vessels and substituted by permanent bone (Anderson and Parker, 1966). In *Rana Esculenta*, the mineralized cartilage was never invaded by vessels nor is the bone substituted.

No evidence of mineralization was present in metaphysis-bone marrow boundary zone.

In mammals, the mineralization of the deeper articular cartilage is typically limited to bone contact layer (Meachim and Stockwell, 1973) and so the bone vessels make Calcium and Phosphate supply possible. In amphibians the articular cartilage is in direct contact with the resting metaphyseal zone and in this region no vascular presence may be evidenced: thus, cartilage mineralization is completely independent from vascular invasion.

With regard to the wedge-shaped area in the metaphysis, the mineralized cartilage was not invaded by vessels and was permanent.

All regions of epiphyseal apparatus were completely negative to 0.6 M $MgCl_2$ Alcian blue: this histochemical evidence demonstrates that keratan-sulphate-containing proteolgycans are completely lacking (Scott and Dorling, 1965). The proteoglycan pattern does not modify from resting to degenerative zone. In mammals, the alcianophylia decreases from resting to calcifying (Poole et al., 1989). In mammals, degenerative cartilage mineralizes and is easily invaded by vessels (Hunter and Arsenault, 1990) and the keratan-sulphate concentration increases from proliferative zone to degenerative one (Dell'Orbo et al., 1982). The cornea contains a little amount of keratan-sulphate (Balduini et al., 1989) and is not invaded by vessels.

So it is possible to suppose that in ranid frog the absence of vascular invasion may be related to the lacking of keratan-sulphate containing proteoglycans.

The absence of vascular invasion might also be caused, in boundary zone, by the limiting cells easily evident by light microscopy in borderline zone between metaphyseal cartilage and bone marrow.

The diaphyseal long bone was completely lacking in osteonic structure and even if sometimes occasional vessels run parallel to the long axis of the diaphysis inside bone tissue, no osteonic organization was evident around them. The complete lack in osteonic bone was not completely unexpected, if the absolute absence of vascular invasion is considered.

The bone diameter enlarged during ageing but the diameter of medullary cavity did not vary significatively: the thickening of diaphyseal bone was the really responsible for diaphysis enlargement. The periosteal layer was probably responsible for new bone deposition.

The periosteum, and particularly the one adjacent to the epiphyseal edge, was the richest in vessels and in cuboidal cells (osteoblasts) and is the most likely for bone lengthening and growth.

The absence of polynucleated osteoclasts and bone resorption lacunae do not permit us to describe bone resorption pictures.

It is possible to suppose that endochondral ossification is an unknown system for the femur of ranid frog and that the growth of long bones in this family is completely supported by mantellar (periosteal) ossification.

Acknowledgements. The authors thank Mr A. Cadau and Mr. Z. Porru for the fine technical assistance. This study was supported by grants from M.U.R.S.T. and C.N.R., Rome, Italy

References

Anderson C.E. and Parker J. (1966). Invasion and resorption in endochondral ossification. J. Bone and Joint Surg. 48 A, 899-913.

Balduini C., De Luca G.C. and Castellani A.A. (1989). Biosynthesis of skeletal and corneal keratan sulphate. In: Keratan Sulphate, chemistry, biology, chemical pathology. (H. Greiling and J.E. Scott eds), The Bioch. Soc. London. 53-66.

De Bernard B., Bianco P., Bonucci E., Costantini M., Lunazzi G.C., Martinuzzi P., Modricky C., Moro L., Panfili E.P., Polesello P., Stagni N. and Vittur F. (1986). Biochemical and immunohystochemical evidence that in cartilage alkaline phosphatase is a Ca ++ binding glycoprotein. J. Cell Biol. 103, 1615-1623.

Dell'Orbo C., Quacci D. and Pazzaglia U.E. (1982). The role of proteoglycans at the beginning of the calcification process: histochemical and ultrastructural observations. Bas. Appl. Hystochem. 26, 35-46.

Dickson G.R. (1978). Ultrastructural localization of alkaline phosphatase in the hypertrophic chondrocyte in the frog. Histochem. 57, 343-347.

Dickson G.R. (1982). Ultrastructure of growth cartilage in the proximal femur of the frog, *Rana temporaria*. J. Anat. 135, 549-564.

Frobose H. (1927). Der Aufbau der Skeletteile in den frein Gliedmassen der anuren Amphibien. Jahr. Morphol. Mikrosk. Anat. 58, 473-566.

Howlett C.R. (1979). The fine structure of the proximal growth plate of the avian tibia. J. Anat. 128, 377-399.

Hunter W.L. and Arsenault A.L. (1990). Vascular invasion of the epiphyseal growth plate: analysis of metaphyseal capillary ultrastructure and growth dinamics. Anat. Rec. 227, 223-231.

Jee W.S.S. (1986). The skeletal tissues. In: Cell and tissue biology (L. Weiss ed.) Urban and Schwarzenberg, Baltimore 213-253.

Landis W.J. and Hodgens K.J. (1980). Visualization of sulfur-containing components associated with proliferating chondrocytes from rat epiphyseal growth plate cartilage: possible proteoglycan and collagen co-migration. Anat. Rec. 226, 153-167.

Meachim G. and Stockwell R.A. (1973). The matrix. In: Adult cartilage (M.R.A. Freeman ed.) Pitman medical, London. 1-50.

Pearse A.G.E. (1980). Histochemistry: theoretical and applied (Churchill Livingstone ed.) Edimburg, London, Melbourne, New York.

Poole A.R., Matzui Y., Hinek A. and Lee E.R. (1989). Cartilage macromolecule and the calcification of cartilage matrix. Anat. Record 224, 167-169.

Quacci D., Dell'Orbo C. and Pazzaglia U.E. (1990). Morphological aspects of rat metaphyseal cartilage pericellular matrix. J. Anat. 171, 193-205.

Reynolds E.S. (1963). The use of lead citrate at high pH as an electron-opaque stain in electron microscopy. J. Cell Biol. 17, 208-212.

Riva A. (1974). A simple and rapid staining method for enhancing the contrast of tissue previously treated with uranyl acetate. J. de Microscopie. 19, 105-108.

Scott J.E. and Dorling J. (1965). Differential staining of acid glycosaminoglycans (mucopolysaccharides) by Alcian blue in salt solutions. Histochemie 5, 221-233.

Scott J.E. and Burton S.M. (1984). Selective demineralization of hard tissues in organic solvents. Retention or extraction of proteoglycans. J. Microscopy 134, 291-297.

Stagni N., Furlan G., Vittur F., Zanetti M. and De Bernard B. (1979). Enzymatic properties of the Ca ++ bund glycoprotein isolated from preosseous cartilage. Calc. Tiss. Int. 29, 27-32.

Thyberg J., Lohmander S. and Friberg U. (1973). Electron microscopic demonstration of proteoglycans in guinea pig epiphsyeal cartilage. J. Ultrastr. Res. 45, 407-427.

Accepted October 25, 1991